Amino Acids (2014) 46:2517–2530
DOI 10.1007/s00726-014-1806-z

ORIGINAL ARTICLE

Structure–activity relationships in ultrashort cationic lipopeptides: the effects of amino acid ring constraint on antibacterial activity

Ronald Domalaon · Xuan Yang · Joe O'Neil · George G. Zhanel · Neeloffer Mookherjee · Frank Schweizer

Received: 29 January 2014 / Accepted: 4 July 2014 / Published online: 29 July 2014

Abstract Taking a minimalistic approach in efforts to lower the cost for the development of new synthetic antimicrobial peptides, ultrashort cationic lipopeptides were designed to mimic the amphiphilic nature crucial for their activity but with only a very short peptide sequence ligated to a lipidic acid. Nine ultrashort cationic lipopeptides were prepared to study the effects of ring constraint in the amino acid side chain of the peptide component. USCL-$P_{Cat}1$, consisting of only four L-4*R*-aminoproline residues and acylated with palmitic acid at the N-terminus, was found to populate a polyproline II helical secondary conformation that is stable to different pHs and temperatures using circular dichroism. The synthesized lipopeptides were found to have a micellar structure in water using negative staining transmission electron microscopy. We found that constraining the side chain of the amino acid component is not beneficial to the antimicrobial activity. USCL-Dab1, USCL-Dab3 and USCL-K1 showed promising activity against a panel of laboratory reference and clinically isolated Gram-positive and Gram-negative bacterial strains, some of which are multidrug resistant. No appreciable cytotoxicity against human monocytic THP-1 cells was observed up to concentrations of 20–40 μM for all synthesized compounds. Moreover, all USCLs did not induce the production of either pro-inflammatory cytokines or chemokines up to 40 μM.

Keywords Antimicrobial peptides · Ultrashort cationic lipopeptides · Polyproline II helix · Circular dichroism · Cationic amphiphiles

R. Domalaon · X. Yang · J. O'Neil · F. Schweizer (✉)
Department of Chemistry, University of Manitoba, Winnipeg, MB R3T 2N2, Canada
e-mail: schweize@cc.umanitoba.ca

G. G. Zhanel · F. Schweizer
Department of Medical Microbiology, University of Manitoba, Winnipeg, MB R3E 0J9, Canada

N. Mookherjee
Departments of Internal Medicine and Immunology, University of Manitoba, Winnipeg, MB R3E 0T5, Canada

Introduction

Drug-resistant bacteria have tremendously increased in the past decade, resulting from selective pressure induced by inappropriate antibiotic use, rendering most of our conventional antimicrobial agents ineffective (Yoneyama and Katsumata 2006; Choe 2012; Stanton 2013). Unfortunately, the pharmaceutical industry has been slow in producing novel antimicrobial agents, partly due to unfavorable economic and regulatory environments (Eisenstein and Hermsen 2012; Jabes 2011), leading to a shortage in our drug arsenal.

Antimicrobial peptides (AMPs), consisting of 12–50 amino acids which usually are cationic, are a promising class of naturally occurring biological molecules to combat drug-resistant microbes due to their multiple modes of action (Findlay et al. 2010). It is widely accepted that lysis or increased permeability of the overall anionic bacterial membrane is the principal mode of action for most AMPs, initially starting from electrostatic interaction with lipopolysaccharide (in Gram-negative) or lipoteichoic acid (in Gram-positive) (Kang et al. 2012) leading to membrane perforation and cell death. In addition, many AMPs can traverse through the cell membrane via self-promoted uptake and interact with cytoplasmic or intracellular anionic molecules such as DNA and autolysins (Hancock and Scott 2000). These multiple modes of action result in

difficulty for microbes to acquire resistance against AMPs. Recently, some AMPs (Steinstraesser et al. 2011; Mookherjee et al. 2007; Choi et al. 2012) and their synthetic mimics (Thaker et al. 2012) are also found to exhibit host-beneficial immunomodulatory effects (induce anti-inflammatory and/or inhibit pro-inflammatory chemokine production in immune cells). Furthermore, not only Gram-positive and Gram-negative microbes, but also viruses, fungi, protozoa and tumor cells are susceptible to AMPs (Yeung et al. 2011).

Lipopeptides represent an amphiphilic class of AMPs where a polar peptide-based head group, typically cyclic, is conjugated to a hydrophobic lipid tail. FDA-approved lipopeptide-based AMPs such as daptomycin, polymyxin B, colistin and ramoplanin are used in clinical settings to treat complicated bacterial infections (Schneider et al. 2013), and other than daptomycin are primarily utilized as topical antimicrobial agents due to their systemic toxicity. Taking a minimalistic approach to AMPs, in efforts to decrease the cost of production and toxicity, ultrashort cationic lipopeptides (USCLs) were designed to have a very short linear peptide-based head of less than five amino acids long. Recent work has shown that USCLs, along with their peptidomimetic analogs (lipo-β-peptides and lipopeptoids), are potent mimics of AMPs as they exhibit similar antimicrobial, antifungal and immunomodulatory properties compared to their longer AMP counterparts (Makovitzki et al. 2006; Laverty et al. 2010; Ahn et al. 2013; Serrano et al. 2009; Findlay et al. 2012b, 2013). In fact, USCLs can display comparable antimicrobial activity against multi-resistant microbes such as methicillin-resistant *Staphylococcus aureus* (MRSA) and methicillin-resistant *Staphylococcus epidermidis* (MRSE) when compared to widely used antiseptics like benzalkonium chloride (Findlay et al. 2012a).

To the best of our knowledge, all USCLs previously reported possess a flexible peptide backbone, prompting our research group to seek conformationally constrained analogs to diversify the USCL design. We decided to use L-proline as an amino acid template due to its ring-constrained side chain. It is known that oligoproline sequences in polar solvents and physiological environments (pH and temperature) adopt a stable left-handed polyproline II (PPII) helical secondary structure, having three residues per turn with a helical pitch of approximately 10 Angstroms (Adzhubei and Sternberg 1993; Adzhubei et al. 2013; Owens et al. 2010). Therefore, we expect our proline-based USCLs to populate an extended PPII helical conformation. Herein, we report the effects of ring-constrained amino acids to the antimicrobial and immunomodulatory properties of USCL. Furthermore, we examined the secondary structure and solution morphology of these USCLs, having a peptide head of only four amino acids long fused to a sixteen carbon-length lipid tail.

Experimental

Materials

Fmoc MBHA Rink amide resin was obtained from Novabiochem (USA). Fmoc-Dab(Boc)-OH, Fmoc-Hyp(tBu)-OH and Fmoc-Lys(Boc)-OH were purchased from Bachem (Switzerland). Fmoc-HoSer(Trt)-OH was obtained from Chem-Impex (USA) while the coupling reagent, *O*-(benzotriazol-1-yl)-*N*,*N*,*N*′,*N*′-tetramethyluronium tetrafluoroborate (TBTU), was purchased from AK Scientific (USA). All other reagents and solvents, unless specified, were purchased from commercially available sources and used without further purification.

Peptide synthesis

All lipopeptides were synthesized on solid-phase support employing fluorenylmethyloxycarbonyl (Fmoc) chemistry (Chan and White 2000). Synthesis was carried out on a GL-25 50 mL peptide vessel from Chemglass (USA). Amino acid building blocks with reactive functional group at its side chain were protected with carefully chosen protecting group that is stable to conditions during deprotection and coupling steps but is labile to conditions during the cleavage step. Hence, protecting groups that are stable to basic conditions and labile to acidic conditions were used. Each lipopeptide sequence was purified via reverse-phase flash chromatography, using C18 (40–63 μm) silica gel from Silicyle (USA). Purity was assessed by HPLC to be >98 %. ^{1}H and ^{13}C nuclear magnetic resonance (NMR) on a Bruker AMX-500 or AMX 300 (Germany) and electrospray ionization mass spectrometry (ESI–MS) on a Varian 500-MS IT mass spectrometer (USA) were used to characterize and confirm the purity of each USCL.

USCL structural studies

Far-ultraviolet circular dichroism (CD) was performed on a JASCO Model J-810 spectropolarimeter (USA). Purified USCL-K1, USCL-Dab1 and USCL-P_{Cat}1 were dried in vacuo for at least 24 h prior to weighing. They were dissolved in 5.0 mL of 10 mM phosphate buffer pH 7.3 to yield either a 500 μM or 50 μM USCL solution. They were then equilibrated for at least 24 h. The pH of the prepared solutions was determined to be neutral (pH ~ 7) at 25 °C. Aliquots were placed in a 0.05 or 0.1 cm path length quartz cell obtained from Hellma Analytics (Germany). Measurements were obtained from 180 to 250 nm with data pitch of 0.1 nm in continuous scanning mode with a speed of 5 nm/min and a response time of 8 s. pH adjustments were carried out by adding a minimum amount of diluted formic acid (25 %) or diluted sodium hydroxide (25 %) to

the prepared solution. Thermal denaturation studies were performed using the 500 μM USCL solution and similar data acquisition method. The temperature was raised stepwise from 5 to 85 °C, in 10 °C interval, and spectra were acquired from 185 to 250 nm. Mean residue ellipticity (MRE) was obtained for the three lipopeptide solutions by employing the formula

$$\mathrm{MRE} = (\theta)(M_r)/(10\ cln)$$

where θ is the CD signal (millidegrees), c is the lipopeptide concentration (g/L), l is the path length of the cuvette (cm), M_r is the relative atomic mass of the lipopeptide and n is the number of amino acid residues in the peptide sequence.

Visualization of USCLs via transmission electron microscopy (TEM) was performed on a Hitachi scanning/transmission electron microscope (STEM) model H-7000 equipped with a Tungsten filament (Japan). Micrographs were obtained using advanced microscopy techniques (AMT) CCD Camera Model 1600M (USA). Each of the USCLs, at 200 μM concentration in water, was vortexed for 5 s and sonicated for 3 s prior to visualization to prevent agglomeration. They were immobilized on a carbon-coated copper grid obtained from Cedarlane (Canada) and were stained using 1 % phosphotungstic acid to visualize their morphology at 60,000X magnification.

Antimicrobial activity measurements

Each purified USCL was tested to obtain minimum inhibitory concentration (MIC in μg/mL) against a panel of standard laboratory reference and clinically isolated bacterial strains using Clinical and Laboratory Standards Institute (CLSI) macrobroth methods (Wayne:CLSI 2006). Stock solutions of 512 μg/mL were prepared using water and testing was performed in glass test tubes using Mueller–Hinton Broth (MHB), with or without the presence of 4 % Bovine Serum Albumin (BSA), containing an inoculum of 5×10^5 colony-forming units (CFU)/mL. The MIC solution contained 90 % MHB with 10 % USCL in water. BSA was used to assess the extent of protein binding of each purified USCL. An MIC increase of 0–4 fold in the presence of BSA (compared to non-BSA control) was considered to demonstrate little to no protein binding while an MIC increase of ≥eightfold was considered to possess significant protein binding. Test organisms were incubated with USCL for 24 h at 37 °C prior to reading. Reference strains including *Staphylococcus aureus* ATCC 29213, methicillin-resistant *S. aureus* (MRSA) ATCC 33592, *Enterococcus faecalis* ATCC 29212, *Enterococcus faecium* ATCC 27270, *Streptococcus pneumoniae* ATCC 49619, *Escherichia coli* ATCC 25922, *Pseudomonas aeruginosa* ATCC 27853 and *Klebsiella pneumoniae* ATCC 13883 were acquired from the American Type Culture Collection (ATCC) and were used as a quality control strains. The clinical strains methicillin-resistant *Staphylococcus epidermidis* (MRSE-cefazolin MIC >32 μg/mL) CAN-ICU 61589, gentamicin-resistant *E. coli* CAN-ICU 61714, Amikacin-resistant (MIC = 32 μg/mL) *E. coli* CAN-ICU 63074, gentamicin-resistant *P. aeruginosa* CAN-ICU 62584, *Strenotrophomonas maltophilia* CAN-ICU 62584 and *Acinetobacter baumannii* CAN-ICU 63169 were obtained from hospitals across Canada as a part of the Canadian National Intensive Care Unit (CAN-ICU) study (Zhanel et al. 2008). Methicillin-susceptible *S. epidermidis* (MSSE) CANWARD-2008 81388 was obtained from the 2008 Canadian Ward Surveillance (CANWARD) study (Zhanel et al. 2010), while gentamicin-resistant tobramycin-resistant ciprofloxacin-resistant [aminoglycoside modifying enzyme aac(3′)-IIa present] *E. coli* CANWARD-2011 97615 and gentamicin-resistant tobramycin-resistant *P. aeruginosa* CANWARD-2011 96846 were obtained from the 2011 CANWARD study (Zhanel et al. 2013).

Cytotoxicity and cytokine measurements

Human monocytic THP-1 cells (ATCC TIB-202) were cultured in RPMI 1640 medium supplemented with 1 mM sodium pyruvate and 10 % (v/v) fetal bovine serum. The cells were maintained at 37 °C in a 5 % CO_2 humidified incubator and differentiated into plastic-adherent macrophage-like cells with phorbol-12-myristate-13-acetate (PMA) obtained from Sigma-Aldrich (Canada) as previously described (Mookherjee et al. 2006). The plastic-adherent cells were rested for 24 h prior to stimulation with the peptides. The peptides were re-suspended in sterile endotoxin-free water before use. Tissue culture (TC) supernatants were collected after 24 h and centrifuged at $250\times g$ for 5 min to obtain cell-free samples. Cellular cytotoxicity was determined by monitoring the release of the enzyme lactate dehydrogenase in the TC supernatants using a colorimetric detection assay from Roche Diagnostic (Canada) as previously described by us (Mookherjee et al. 2006; Turner-Brannen et al. 2011). Production of chemokines, TNF-α and IL-1β, was monitored in the TC supernatants using specific antibody pairs from eBiosciences (USA), and chemokines Gro-a and IL-8 were monitored using antibody pairs from R&D Systems (USA), by enzyme-linked immunosorbent assay (ELISA) as per the manufacturers' instructions. Serial dilutions of the recombinant human cytokines and chemokines were used to establish a standard curves for the evaluation of the cytokine concentrations in the TC supernatants. Results shown are an average of three independent experiments ± standard error. The p values were calculated using a Student's paired t test, and results with $p < 0.05$ were considered to be statistically significant.

Synthesis of proline-modified amino acids

*(2S,4R)-N$^{\alpha}$-Cbz-4-hexyloxyproline (**2**)*

20 mL of *N*,*N*-dimethylformamide (DMF) was added to a flask (preflushed) containing L-*N*$^{\alpha}$-Cbz-4-hydroxyproline (**1**) (1.076 g, 4.0 mmol) and 60 % sodium hydride (0.824 g, 21.5 mmol) in an ice bath under N_2 atmosphere. The mixture was stirred for 5 min, then followed by the addition of 1-bromohexane (1.8 mL, 12.8 mmol). The solution was gradually warmed to room temperature while stirring for 19 h. In an ice bath under N_2 atmosphere, saturated ammonium chloride followed by 1 M HCl was slowly added to acidify the solution to pH 4–5. Extraction was performed using dichloromethane (DCM). The organic layer was washed with water and dried using anhydrous sodium sulfate. The solvent was removed in vacuo followed by purification using flash chromatography (eluent, chloroform/methanol = 20:1) to afford a yellow oil (**2**). Yield: 1.050 g (74 %). ^{1}H NMR (300 MHz, $CDCl_3$, rotamers present) δ = 7.44–7.25 (m, 5H, benzyl aromatic), 5.28–5.05 (m, 2H, benzyl –O–CH_2–), 4.58–4.43 (m, 1H, Pro_{α}), 4.16–4.06 (m, 1H, Pro_{γ}), 3.78–3.56 (m, 2H, Pro_{δ}), 3.49–3.34 (m, 2H, hexyl –O–CH_2–), 2.50–2.11 (m, 2H, Pro_{β}), 1.64–1.47 (m, 2H, hexyl–CH_2–), 1.35–1.26 (m, 6H, hexyl–CH_2–), 0.91 (t, J = 7.2, 3H, hexyl–CH_3). ^{13}C NMR (75 MHz, $CDCl_3$, rotamers present) δ = 177.92, 176.91, 156.44, 154.68, 136.30, 128.75, 128.69, 128.61, 128.41, 128.14, 128.10, 127.99, 127.83, 76.90, 76.46, 69.74, 67.97, 67.48, 58.41, 57.79, 52.18, 52.02, 36.95, 35.12, 31.80, 29.90, 25.96, 22.78, 14.23. MS (ESI) *m*/*z* calcd for $C_{19}H_{27}NO_5Na$ $(M+Na)^+$: 372.18, found: 372.3. R_f = 0.42 (DCM/MeOH = 9:1).

(2S,4R)-N$^{\alpha}$-Fmoc-4-hexyloxyproline (Fmoc-P_{Hex}-OH)

Compound **2** (1.702 g, 4.9 mmol) was dissolved in methanol (25 mL). 10 % Pd on carbon (125 mg) was added and the reaction flask was subjected to catalytic hydrogenation via H_2 balloon for 6.5 h. The solution was filtered through Celite and washed with methanol. Solvent was evaporated in vacuo to afford the crude-free amine product, used in the next step without further purification. A portion of the crude (0.252 g, 1.1 mmol) and sodium bicarbonate (0.230 g, 2.7 mmol) was suspended in water (5 mL) and immersed in an ice bath. Fmoc-Cl (0.421 g, 1.6 mmol) dissolved in dioxane (2.5 mL) was added to the reaction flask. The solution was warmed to room temperature while stirring for 2.5 h. Water (10 mL) was added to dilute the solution followed by acidification using acetic acid to pH 4. Extraction was done using ethyl acetate (EtOAc). The organic layer was washed with brine and dried using anhydrous sulfate. The solvent was removed in vacuo followed by purification using flash chromatography (eluent, chloroform/methanol = 20:1) to afford a pale yellow viscous oil (**3**). Yield: 0.398 g (82.3 %). ^{1}H NMR (300 MHz, $CDCl_3$, rotamers present) δ = 7.76 (dd, J = 15.7, 7.6, 2H, Fmoc aromatic), 7.64–7.49 (m, J = 13.8, 6.8, 2H, Fmoc aromatic), 7.47–7.29 (m, 4H, Fmoc aromatic), 4.54–4.02 (m, 5H, Pro_{α} + Pro_{γ} + Fmoc –O–CH_2–CH–), 3.80–3.51 (m, 2H, Pro_{δ}), 3.51–3.29 (m, 2H, hexyl –O–CH_2–), 2.50–2.08 (m, 2H, Pro_{β}), 1.62–1.46 (m, 2H, hexyl–CH_2–), 1.39–1.28 (m, 6H, hexyl–CH_2–), 0.95–0.86 (m, 3H, hexyl–CH_3). ^{13}C NMR (75 MHz, $CDCl_3$, rotamers present) δ = 177.49, 175.59, 156.13, 154.60, 144.04, 143.76, 143.71, 141.31, 127.78, 127.64, 127.10, 125.07, 124.95, 120.02, 119.90, 69.55, 69.51, 68.07, 67.71, 58.25, 57.51, 52.01, 51.81, 47.21, 47.12, 36.90, 34.92, 31.64, 29.76, 25.82, 22.61, 14.05. MS (ESI) *m*/*z* calcd for $C_{26}H_{31}NO_5Na$ $(M+Na)^+$: 460.21, found: 460.5. R_f = 0.46 (DCM/MeOH = 9:1).

*(2S,4R)-N$^{\alpha}$-Cbz-4-hydroxyproline benzyl ester (**3**)*

DMF (20 mL) was added to a flask containing L-*N*$^{\alpha}$-Cbz-4-hydroxyproline (**1**) (3.065 g, 11.5 mmol) and cesium carbonate (7.588 g, 23.3 mmol) in an ice bath. Benzyl bromide (1.8 mL, 15.2 mmol) was then slowly added while stirring. The solution was further stirred for 2 h. It was then warmed to room temperature and filtered through Celite, followed by successive washings with EtOAc. The solvent was evaporated in vacuo followed by purification using flash chromatography (eluent, hexanes/EtOAc = 3:2) to give a pale yellow oil (**4**). Yield: 3.201 g (78 %). ^{1}H NMR (300 MHz, $CDCl_3$, rotamers present) δ 7.66–6.95 (m, 10H, benzyl aromatic), 5.32–4.91 (m, 4H, benzyl –O–CH_2–), 4.63–4.49 (m, 1H, Pro_{α}), 4.48–4.36 (m, 1H, Pro_{γ}), 3.72–3.50 (m, 2H, Pro_{δ}), 2.38–2.20 (m, 1H, $Pro_{\beta1}$), 2.13–1.97 (m, 1H, $Pro_{\beta2}$). ^{13}C NMR (75 MHz, $CDCl_3$, rotamers present) δ = 172.76, 172.56, 155.25, 154.79, 136.47, 136.25, 135.64, 135.42, 128.64, 128.56, 128.50, 128.45, 128.36, 128.21, 128.16, 128.12, 128.08, 127.91, 127.85, 69.93, 69.20, 67.37, 67.04, 66.92, 58.21, 57.97, 55.28, 54.70, 39.16, 38.37. MS (ESI) *m*/*z* calcd for $C_{20}H_{21}NO_5Na$ $(M+Na)^+$: 378.13, found: 378.5. R_f = 0.21 (hexanes/EtOAc = 1:1).

*(2S,4S)-N$^{\alpha}$-Cbz-4-bromoproline benzyl ester (**4**)*

Compound **3** (3.200 g, 9.0 mmol) was dissolved in DCM (35 mL) and cooled in an ice bath. Carbon tetrabromide (11.814 g, 35.6 mmol) and triphenylphosphine (8.956 g, 34.2 mmol) were added to the solution and stirred for 30 min. It was then warmed to room temperature gradually while stirring. After 6 h, ethanol (8 mL) was added and the solution was further stirred for another 18 h. Diethyl ether was added, which resulted in precipitate formation. The reaction mixture was filtered through Buchner filtration to give a clear pale yellow solution. The solvent

was removed in vacuo followed by purification using flash chromatography (eluent, hexanes/EtOAc = 2:1) to give a white solid product (**5**). Yield: 3.648 g (97 %). ^{1}H NMR (300 MHz, $CDCl_3$, rotamers present) δ = 7.48–7.20 (m, 10H, benzyl aromatic), 5.36–4.98 (m, 4H, benzyl –O–CH_2–), 4.62–4.43 (m, 1H, Pro_α), 4.33 (p, J = 6.0, 1H, Pro_γ), 4.23–4.05 (m, 1H, $Pro_{\delta1}$), 3.94–3.75 (m, 1H, $Pro_{\delta2}$), 2.93–2.75 (m, 1H, $Pro_{\beta1}$), 2.59–2.42 (m, 1H, $Pro_{\beta2}$). ^{13}C NMR (75 MHz, $CDCl_3$, rotamers present) δ = 171.21, 170.95, 154.39, 153.92, 136.33, 136.26, 135.53, 135.36, 128.66, 128.57, 128.51, 128.43, 128.37, 128.28, 128.19, 128.13, 128.02, 67.56, 67.49, 67.35, 67.29, 58.53, 58.30, 56.04, 55.67, 42.26, 41.55, 41.02, 39.99. MS (ESI) *m/z* calcd for $C_{20}H_{20}BrNO_4Na$ $(M+Na)^+$: 440.05, found: 440.2. R_f = 0.68 (hexanes/EtOAc = 1:1).

*(2S,4R)-N$^\alpha$-Cbz-4-azidoproline benzyl ester (**5**)*

Compound **4** (6.260 g, 15.0 mmol) was dissolved in DMF (32 mL). Sodium azide (3.076 g, 47.3 mmol) was added to the solution, followed by heating to 75–78 °C for 6 h. Water (120 mL) was added and the resulting mixture was extracted with EtOAc. The organic layer was washed with ample amount of water and dried using anhydrous sodium sulfate. The solvent was removed in vacuo followed by purification using flash chromatography (eluent, hexanes/EtOAc = 3:1) to give a white oil which solidified while standing (**6**). Yield: 4.656 g (82 %). ^{1}H NMR (300 MHz, $CDCl_3$, rotamers present) δ = 7.45–7.21 (m, 10H, benzyl aromatic), 5.27–5.00 (m, 4H, benzyl –O–CH_2–), 4.62–4.46 (m, 1H, Pro_α), 4.27–4.16 (m, 1H, Pro_γ), 3.87–3.52 (m, 2H, Pro_δ), 2.44–2.28 (m, 1H, $Pro_{\beta1}$), 2.28–2.14 (m, 1H, $Pro_{\beta2}$). ^{13}C NMR (75 MHz, $CDCl_3$, rotamers present) δ = 171.98, 171.80, 154.67, 154.11, 136.36, 136.24, 135.50, 135.29, 128.72, 128.63, 128.59, 128.56, 128.50, 128.32, 128.25, 128.18, 128.04, 127.98, 67.55, 67.48, 67.27, 67.16, 59.32, 58.75, 58.05, 57.76, 51.92, 51.43, 36.39, 35.34. MS (ESI) *m/z* calcd for $C_{20}H_{20}N_4O_4Na$ $(M+Na)^+$: 403.14, found: 403.3. R_f = 0.72 (hexanes/EtOAc = 4:3).

*(2S,4R)-N$^\alpha$-Cbz-4-N-Boc-aminoproline benzyl ester (**6**)*

Compound **5** (2.330 g, 6.1 mmol) was dissolved in 20 mL tetrahydrofuran (THF). Triphenylphosphine (4.030 g, 15.4 mmol) and water (0.2 mL, 11.1 mmol) were added to the solution while stirring. The resulting mixture was heated to 73–76 °C for 6 h. The solution was cooled to room temperature, followed by evaporation in vacuo to remove the solvent. The residue was re-dissolved using 25 mL 1 M HCl and 30 mL diethyl ether, and then extracted with diethyl ether. The aqueous layer was neutralized with 10 % sodium carbonate, and then extracted with DCM. The resulting DCM layer was dried using anhydrous sodium sulfate and concentrated to obtain 2.398 g of crude oil. It was then dissolved in THF (8 mL) and stirred. Triethylamine (2.8 mL, 18.6 mmol) and di-tert-butyl dicarbonate (2.670 g, 12.2 mmol) were then added. The resulting solution was stirred for 5.5 h. The solvent was removed in vacuo followed by purification using flash chromatography (eluent, hexanes/EtOAc = 7:3) to afford a white solid (**7**). Yield: 2.306 g (83 %). ^{1}H NMR (300 MHz, $CDCl_3$, rotamers present) δ = 7.42–7.23 (m, 10H, benzyl aromatic), 5.31–5.01 (m, 4H, benzyl –O–CH_2–), 4.57–4.39 (m, 1H, Pro_α), 4.38–4.21 (m, 1H, Pro_γ), 3.92–3.78 (m, 1H, $Pro_{\delta1}$), 3.52–3.32 (m, 1H, $Pro_{\delta2}$), 2.31–2.15 (m, 2H, Pro_β), 1.45 (s, 9H, Boc –CH_3). ^{13}C NMR (75 MHz, $CDCl_3$, rotamers present) δ = 172.15, 171.90, 155.27, 155.24, 154.95, 154.30, 136.50, 136.34, 135.60, 135.42, 128.74, 128.65, 128.59, 128.56, 128.47, 128.34, 128.26, 128.23, 128.20, 128.05, 128.03, 80.14, 67.44, 67.40, 67.23, 67.12, 58.08, 57.83, 52.40, 52.13, 49.75, 49.18, 37.11, 35.98, 28.48. MS (ESI) *m/z* calcd for $C_{25}H_{30}N_2O_6Na$ $(M+Na)^+$: 477.20, found: 477.4. R_f = 0.47 (hexanes/EtOAc = 3:3).

*(2S,4R)-N$^\alpha$-Fmoc-4-N-Boc-aminoproline (Fmoc-P_{Cat}-OH) (**8**)*

Compound **6** (1.826 g, 4.020 mmol) was dissolved in 1:3 THF/methanol (40 mL). 10 % Pd on carbon (320 mg) was added and the reaction flask was subjected to catalytic hydrogenation via H_2 balloon for 21.5 h. The solution was filtered through Celite and washed with methanol. Solvent was evaporated in vacuo to afford the crude-free amine product, used in the next step without further purification. The crude was dissolved in 10:3 water/THF (65 mL). Triethylamine (1.2 mL, 8.6 mmol) was added to the solution while stirring in an ice bath. Fmoc-OSu (1.977 g, 5.9 mmol) dissolved in dioxane (9 mL) was added to the reaction flask. The solution was warmed to room temperature while stirring for 5 h. The solution was acidified to pH 4 using acetic acid. Solvent was evaporated in vacuo to remove any presence of THF. Extraction was performed using EtOAc. The organic layer was washed with brine and dried using anhydrous sulfate. The solvent was removed in vacuo followed by purification using flash chromatography (eluent, chloroform/methanol = 20:1) to afford a white foam (**8**). Yield: 1.450 g (80 %). ^{1}H NMR (300 MHz, $CDCl_3$, rotamers present) δ = 7.74 (dd, J = 13.2, 7.6, 2H, Fmoc aromatic), 7.57 (dd, J = 17.2, 5.7, 2H, Fmoc aromatic), 7.46–7.25 (m, 4H, Fmoc aromatic), 4.53–4.05 (m, 5H, Pro_α + Pro_γ + Fmoc –O–CH_2–CH–), 3.88–3.77 (m, 1H, $Pro_{\delta1}$), 3.43–3.25 (m, 1H, $Pro_{\delta2}$), 2.50–2.06 (m, 2H, Pro_β), 1.57–1.36 (m, 9H, Boc –O–CH_3). ^{13}C NMR (75 MHz, $CDCl_3$, rotamers present) δ = 175.88, 175.00, 155.67, 154.67, 144.18, 144.07, 143.84, 143.80, 141.50, 141.45, 127.94, 127.86, 127.32, 127.24, 125.28, 125.23, 125.17, 120.15, 80.44, 68.10, 67.93, 58.11, 57.61, 52.20,

49.85, 48.87, 47.38, 47.33, 37.12, 35.62, 28.55. MS (ESI) *m/z* calcd for $C_{25}H_{28}N_2O_6Na$ $(M+Na)^+$: 475.18, found: 475.4. $R_f = 0.53$ (DCM/methanol = 9:1).

Synthesized USCLs

C16-KKKK

^{1}H NMR (500 MHz, methanol-d) δ 4.35–4.18 (m, 4H, K_α), 2.98–2.84 (m, 8H, K_ε), 2.28–2.19 (m, 2H, C16 –CO–CH_2–), 1.88–1.25 (m, 50H, $K_\beta + K_\gamma + K_\delta$ + C16 aliphatic –CH_2–), 0.88 (t, $J = 6.9$ Hz, 3H, C16 –CH_3). ^{13}C NMR (126 MHz, methanol-d) δ 176.76, 176.57, 174.84, 174.37, 173.99, 55.10, 54.79, 54.67, 54.24, 40.58, 40.53, 40.49, 40.44, 36.74, 33.06, 32.57, 32.54, 32.18, 32.12, 32.04, 30.79, 30.77, 30.76, 30.75, 30.67, 30.48, 30.46, 30.41, 28.09, 28.00, 27.92, 27.91, 26.92, 23.89, 23.75, 23.72, 23.66, 21.36, 14.43. MS (ESI) *m/z* calcd for $C_{40}H_{82}N_9O_5$ $(M+H)^+$: 769.14 found: 768.9.

C16-Dab-Dab-Dab-Dab

^{1}H NMR (300 MHz, methanol-d) δ 4.51–4.31 (m, 4H, Dab_α), 3.19–2.86 (m, 8H, Dab_γ), 2.32–1.99 (m, 10H, Dab_β + C16 –CO–CH_2–), 1.68–1.53 (m, 2H, C16 aliphatic –CH_2–), 1.37–1.22 (m, 24H, C16 aliphatic –CH_2–), 0.90 (t, $J = 6.8$ Hz, 3H, C16 –CH_3). ^{13}C NMR (75 MHz, methanol-d) δ 177.08, 174.92, 173.74, 173.15, 172.93, 52.73, 52.66, 52.62, 52.03, 37.69, 36.72, 33.05, 31.18, 30.77, 30.75, 30.63, 30.44, 28.80, 26.79, 23.70, 20.42, 14.41. MS (ESI) *m/z* calcd for $C_{32}H_{65}N_9O_5Na$ $(M+Na)^+$: 678.91 found: 678.8.

C16-P_{Cat}-P_{Cat}-P_{Cat}-P_{Cat}

^{1}H NMR (500 MHz, methanol-d, rotamers present) δ 5.01–4.88 (m, 3H, $P_{Cat\ \alpha}$), 4.66–4.53 (m, 1H, $P_{Cat\ \alpha}$), 4.25–3.37 (m, 12H, $P_{Cat\ \gamma} + P_{Cat\ \delta}$), 2.67–2.13 (m, 10H, $P_{Cat\ \beta}$ + C16 –CO–CH_2–), 1.64–1.53 (m, 2H, C16 aliphatic –CH_2–), 1.36–1.25 (m, 24H, C16 aliphatic –CH_2–), 0.90 (t, $J = 6.9$ Hz, 3H, C16 –CH_3). ^{13}C NMR (126 MHz, methanol-d, rotamers present) δ 175.14, 174.53, 174.50, 172.09, 172.06, 171.30, 171.28, 171.13, 171.11, 59.87, 59.48, 58.07, 57.86, 57.50, 51.96, 51.91, 51.74, 51.56, 51.50, 51.39, 51.34, 51.25, 35.18, 34.36, 33.50, 33.19, 33.15, 33.05, 30.77, 30.74, 30.70, 30.62, 30.59, 30.45, 30.40, 30.36, 30.33, 26.93, 25.57, 23.72, 14.42. MS (ESI) *m/z* calcd for $C_{36}H_{65}N_9O_5Na$ $(M+Na)^+$: 726.95 found: 726.7.

C16-Dab-HSe-HSe-Dab

^{1}H NMR (300 MHz, methanol-d) δ 4.53–4.34 (m, 4H, Dab_α + HSe_α), 3.76–3.58 (m, 4H, HSe_γ), 3.13–2.93 (m, 4H, Dab_γ), 2.31–1.90 (m, 10H, Dab_β + HSe_β + C16 –CO–CH_2–), 1.67–1.55 (m, 2H, C16 aliphatic –CH_2–), 1.35–1.25 (m, 23H, C16 aliphatic –CH_2–), 0.90 (t, $J = 6.6$ Hz, 3H, C16 –CH_3). ^{13}C NMR (75 MHz, methanol-d) δ 177.02, 175.12, 174.56, 174.54, 173.35, 59.54, 59.35, 53.51, 53.11, 52.58, 51.81, 49.00, 37.84, 37.68, 36.68, 34.91, 34.84, 33.05, 30.91, 30.77, 30.74, 30.64, 30.53, 30.48, 30.45, 30.42, 26.73, 23.71, 14.41. MS (ESI) *m/z* calcd for $C_{32}H_{64}N_7O_7$ $(M+H)^+$: 658.89 found: 658.9.

C16-P_{Cat}-P_{Hyp}-P_{Hyp}-P_{Cat}

^{1}H NMR (300 MHz, methanol-d, rotamers present) δ 4.84–4.45 (m, 6H, $P_{Hyp\ \gamma} + P_{Cat/Hyp\ \alpha}$), 4.20–3.56 (m, 10H, $P_{Cat\ \gamma} + P_{Cat/Hyp\ \delta}$), 2.66–1.98 (m, 10H, $P_{Cat/Hyp\ \beta}$ + C16 –CO–CH_2–), 1.69–1.53 (m, 2H, C16 aliphatic –CH_2–), 1.40–1.25 (m, 24H, C16 aliphatic –CH_2–), 0.92 (t, $J = 6.8$ Hz, 3H, C16 –CH_3). ^{13}C NMR (75 MHz, methanol-d, rotamers present) δ 175.31, 175.28, 175.15, 174.37, 172.44, 172.28, 172.25, 171.97, 71.07, 71.04, 59.40, 58.89, 58.72, 58.56, 58.35, 57.63, 56.51, 56.45, 56.22, 51.90, 51.50, 51.35, 51.28, 51.19, 37.54, 37.48, 35.26, 34.67, 34.29, 33.47, 33.05, 30.77, 30.74, 30.67, 30.63, 30.59, 30.56, 30.44, 30.36, 26.93, 25.71, 25.61, 23.71, 14.42. MS (ESI) *m/z* calcd for $C_{36}H_{64}N_7O_7Na$ $(M+Na)^+$: 706.94 found: 706.9.

C16-P_{Cat}-P_{Hex}-P_{Hex}-P_{Cat}

^{1}H NMR (300 MHz, methanol-d, rotamers present) δ 4.81–4.55 (m, 4H, $P_{Cat/Hex\ \alpha}$), 4.31–3.35 (m, 18H, $P_{Cat/Hex\ \gamma} + P_{Cat/Hex\ \delta} + P_{Hex}$ –O–CH_2–), 2.50–1.93 (m, 10H, $P_{Cat/Hex\ \beta}$ + C16 –CO–CH_2–), 1.70–0.76 (m, 51H, C16 aliphatic –CH_2– +C16 –CH_3). ^{13}C NMR (75 MHz, methanol-d, rotamers present) δ 175.32, 175.30, 174.27, 174.23, 172.53, 172.26, 172.23, 172.06, 79.06, 78.91, 78.83, 78.74, 70.49, 70.46, 70.37, 70.22, 59.40, 58.77, 58.64, 58.26, 58.20, 53.38, 53.27, 51.69, 51.61, 51.46, 51.34, 35.37, 35.33, 35.26, 35.14, 35.08, 34.66, 34.30, 33.06, 32.93, 32.87, 32.83, 32.79, 32.59, 31.06, 30.88, 30.78, 30.75, 30.62, 30.56, 30.46, 30.34, 30.09, 30.04, 27.05, 26.96, 26.94, 26.67, 25.75, 25.61, 23.71, 23.69, 23.61, 14.43, 14.33. MS (ESI) *m/z* calcd for $C_{48}H_{87}N_7O_7Na$ $(M+Na)^+$: 897.24 found: 897.3.

C16OH-KKKK

^{1}H NMR (300 MHz, methanol-d) δ 4.38–4.21 (m, 4H, K_α), 3.53 (t, $J = 6.6$ Hz, 2H, C160H alkyl –CH_2–OH), 3.09–2.79 (m, 8H, K_ε), 2.24 (t, $J = 7.3$ Hz, 2H, C16OH –CO–CH_2–), 1.89–1.27 (m, 50H, $K_\beta + K_\gamma + K_\delta$ + C16OH aliphatic –CH_2–). ^{13}C NMR (75 MHz, methanol-d) δ 176.73, 176.51, 174.79, 174.32, 173.95, 63.01, 55.07, 54.74, 54.65, 54.22, 40.48, 40.44, 36.74, 33.66, 32.56, 32.21, 32.16, 32.04, 30.74, 30.71, 30.65, 30.58, 30.52, 30.47, 30.40, 30.13, 29.17, 28.09, 28.02, 27.94, 27.92, 26.94,

26.92, 26.61, 23.90, 23.75, 23.65. MS (ESI) *m/z* calcd for $C_{40}H_{81}N_9O_6Na$ $(M+Na)^+$: 807.12 found: 806.9.

C16OH-Dab-Dab-Dab-Dab

^{1}H NMR (300 MHz, methanol-d) δ 4.50–4.36 (m, 4H, Dab_α), 3.54 (t, J = 6.6 Hz, 2H, C160H alkyl $-CH_2-$OH), 3.14–2.96 (m, 8H, Dab_γ), 2.32–2.00 (m, 10H, Dab_β + C16OH $-CO-CH_2-$), 1.64–1.47 (m, 4H, C16OH aliphatic $-CH_2-$), 1.34–1.24 (m, 22H, C16OH aliphatic $-CH_2-$). ^{13}C NMR (75 MHz, methanol-d) δ 177.06, 174.90, 173.72, 173.11, 172.89, 63.01, 52.73, 52.65, 52.63, 52.04, 49.00, 40.06, 37.71, 37.63, 37.49, 36.73, 33.66, 31.20, 31.03, 30.98, 30.75, 30.71, 30.63, 30.59, 30.47, 30.44, 30.25, 28.89, 26.94, 26.80, 25.34, 22.02. MS (ESI) *m/z* calcd for $C_{32}H_{65}N_9O_6Na$ $(M+Na)^+$: 694.90 found: 694.9.

C16OH-P_{Cat}-P_{Cat}-P_{Cat}-P_{Cat}

^{1}H NMR (300 MHz, methanol-d, rotamers present) δ 4.99–4.89 (m, 3H, $P_{Cat\alpha}$), 4.71–4.58 (m, 1H, $P_{Cat\alpha}$), 4.29–3.66 (m, 12H, $P_{Cat\gamma}$ + $P_{Cat\delta}$), 3.56 (t, J = 6.6 Hz, 2H, C160H alkyl $-CH_2-$OH), 2.70–2.28 (m, 10H, $P_{Cat\beta}$ + C16 $-CO-CH_2-$), 1.69–1.49 (m, 4H, C16OH aliphatic $-CH_2-$), 1.39–1.26 (m, 22H, C16OH aliphatic $-CH_2-$). ^{13}C NMR (75 MHz, methanol-d, rotamers present) δ 175.12, 174.53, 172.10, 171.30, 171.12, 63.01, 59.52, 59.49, 58.10, 58.03, 57.88, 57.83, 57.60, 57.50, 51.95, 51.91, 51.74, 51.55, 51.49, 51.36, 51.34, 51.25, 49.00, 35.19, 34.37, 33.65, 33.50, 33.16, 33.02, 30.74, 30.70, 30.59, 30.52, 30.33, 30.13, 29.17, 26.94, 26.61, 25.57. MS (ESI) *m/z* calcd for $C_{36}H_{66}N_9O_6$ $(M+H)^+$: 720.97 found: 720.9.

Results and Discussion

Chemistry

Proline-derivative design

To study how rigidity of the amino acid side chain in L-diaminobutyric acid (Dab) and L-homoserine (HSe) affects the structural and antimicrobial properties of USCLs, we decided to use L-4*R*-aminoproline (P_{Cat}) and L-4*R*-hydroxyproline (P_{Hyp}). Both P_{Cat} and P_{Hyp} are conformationally constrained analogs of Dab and HSe in which the acyclic side chain has been constrained in the form of a five-membered pyrrolidine ring (Fig. 1). To add structural diversity and to explore the effect of increased hydrophobicity, we also prepared L-4*R*-hexyloxy-based proline analog (P_{Hex}). Both P_{Hex} and P_{Cat} were synthesized as shown in Schemes 1 and 2. The synthesized proline-based amino acids P_{Hex} and P_{Cat} were chosen to be Fmoc protected on their N^α since an Fmoc-based strategy will be employed for the solid-phase peptide synthesis of USCLs.

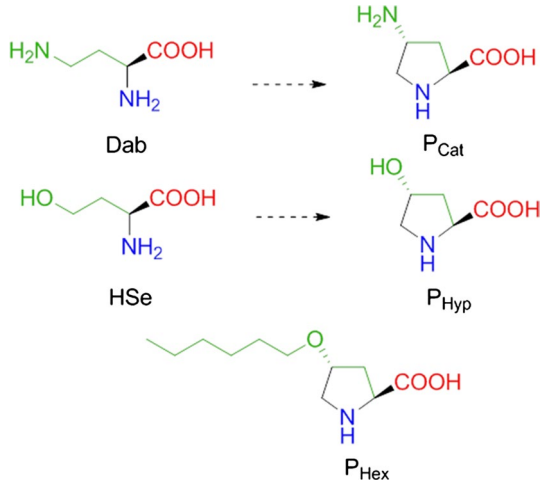

Fig. 1 Replacement of L-diaminobutyric acid (Dab) by L-4*R*-aminoproline (P_{Cat}) or L-homoserine (HSe) by L-4*R*-hydroxyproline (P_{Hyp}) constrains the amino acid side chain in USCL resulting in increased rigidity. P_{Hex} is a lipophilic proline building block used to explore hydrophobic effects in the peptide head portion of the USCL design

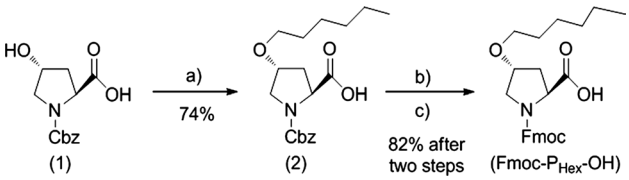

Scheme 1 Synthesis of Fmoc-P_{Hex}-OH. Reagents and conditions; *a* 60 % NaH, 1-bromohexane; *b* 10 % Pd on carbon, H_2; *c* Fmoc-Cl, $NaHCO_3$

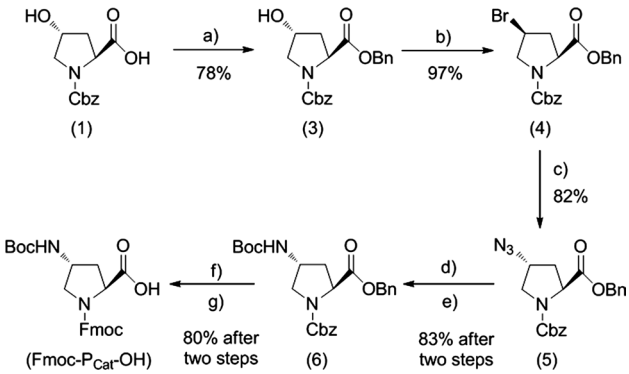

Scheme 2 Synthesis of Fmoc-P_{Cat}-OH. Reagents and conditions; *a* BnBr, Cs_2CO_3; *b* CBr_4, triphenylphosphine; *c* NaN_3; *d* triphenylphosphine, water; *e* di-*tert*-butyl dicarbonate, triethylamine; *f* 10 % Pd on carbon, H_2; *g* Fmoc-OSu, triethylamine

The attachment of a hexyl group to L-N^α-Cbz-4R-hydroxyproline (**1**) was achieved by *O*-alkylation of

1-bromohexane under basic conditions (Scheme 1). Di- and mono-alkylation was observed, as both the hydroxyl and carboxylic acid moiety could serve as nucleophilic centres. The mono-alkylated ether (**2**) was found to be the major product in this condition. Catalytic hydrogenation using 10 % Pd on carbon was performed to remove the Cbz protecting group. The resulting crude material was filtered and used in the next step without further purification. Fmoc-Cl was used to protect the N^{α}, affording the Fmoc-protected P_{Hex} (Fmoc-P_{Hex}-OH) in high yields (82 %).

P_{Cat} was synthesized as shown in Scheme 2. The carboxylic acid functionality of *L*-N^{α}-Cbz-4*R*-hydroxyproline (**1**) was protected in the form of a benzyl ester by alkylation with benzyl bromide to avoid possible side reactions later in the synthesis, using cesium carbonate as a base. To retain the original chirality at the γ-carbon, the hydroxyl group was converted into epimeric bromide (**4**) followed by displacement with sodium azide to afford 4R-azidoproline (**5**), effectively achieving a double inversion. The reduction of the azide was achieved using triphenylphosphine in THF and water followed by Boc protection to produce compound (**6**) in 83 % yield. Other methods for the selective azide reduction such as catalytic hydrogenation and sodium borohydride reduction were deemed unsuitable since the molecule contains other functionalities unstable to such conditions. Both Cbz and benzyl ester protecting groups of the Boc-protected aminoproline were cleaved by hydrogenolysis. The crude product was used in the next step without any purification. The Fmoc protecting group was installed at N^{α} using Fmoc-OSu to yield the building block Fmoc-P_{Cat}-OH in 80 % yield.

USCL design

Table 1 shows all synthesized tetrapeptide-based lipopeptides. USCL-K1 is used as a reference lipopeptide as this sequence's antibacterial activity has been explored previously (Serrano et al. 2009). Three analogous sequences were made to study the effects of ring constraint within the USCL design: USCL-Dab1 versus USCL-P_{Cat}1, USCL-Dab2 versus USCL-P_{Cat}2 and USCL-Dab3 versus USCL-P_{Cat}3. To study how the nature of the lipid tail affects the properties of the lipopeptides USCL-K2, USCL-Dab2 and USCL-P_{Cat}2 bearing 16-hydroxypalmitic acid (C16OH) instead of palmitic acid were prepared. It was expected for the hydroxyl group at the end of the lipid tail to disturb the amphiphilic nature of the USCL design, resulting in significant changes to structural and biological properties. For further variation, we incorporated L-homoserine (HSe) and L-4*R*-hydroxyproline (P_{Hyp}) in the design resulting in the analogous lipopeptide sequence USCL-Dab3 and USCL-P_{Cat}3. We also incorporated P_{Hex} in the design of USCL-P_{Cat}4 to study the hydrophobic effects in the peptide head.

Table 1 Synthesized USCLs (TFA salts)

Code	Compound	Molecular mass (g/mol)
USCL-K1	C16-KKKK-NH_2	1,224.22
USCL-Dab1	C16-DabDabDabDab-NH_2	1,112.01
USCL-P_{Cat}1	C16-$P_{Cat}P_{Cat}P_{Cat}P_{Cat}$-$NH_2$	1,160.05
USCL-K2	C16OH-KKKK-NH_2	1,240.20
USCL-Dab2	C16OH-DabDabDabDab-NH_2	1,128.01
USCL-P_{Cat}2	C16OH-$P_{Cat}P_{Cat}P_{Cat}P_{Cat}$-$NH_2$	1,176.05
USCL-Dab3	C16-DabHSeHSeDab-NH_2	933.97
USCL-P_{Cat}3	C16-$P_{Cat}P_{Hyp}P_{Hyp}P_{Cat}$-$NH_2$	885.93
USCL-P_{Cat}4	C16-$P_{Cat}P_{Hex}P_{Hex}P_{Cat}$-$NH_2$	1,102.29

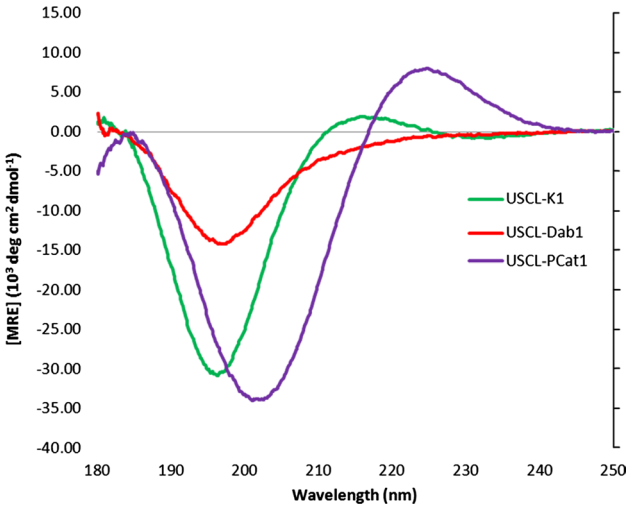

Fig. 2 Molar ellipticity per mean residue for USCL-K1, USCL-Dab1 and USCL-P_{Cat}1 in 10 mM phosphate buffer at 25 °C and neutral pH

Structural studies

An interesting notion that we explored is the ability of these USCLs, which contain a very minimal amount of amino acid, to form secondary structures in water. Moreover, the peptides are acylated with a long aliphatic hydrocarbon chain (C16 or C16OH) that may affect the solution structure via hydrophobic interactions with another lipid tail. Longer AMPs often exhibit α-helical, β-sheet-like or extended secondary structures (Nguyen et al. 2011). For example, the AMP magainin, first isolated from the skin of the African clawed frog *Xenopus laevis* (Zasloff 1987), forms an α-helical structure in trifluoroethanol–water mixture (Haney et al. 2009). Previous studies have shown that separation or segregation of hydrophobic and polar-cationic domains is critical for their antibacterial mode of action (Kang et al. 2012; Hancock and Scott 2000).

Far-ultraviolet circular dichroism spectra were measured for USCL-K1, USCL-Dab1 and USCL-P_{Cat}1 as representative examples among the synthesized USCLs (Fig. 2). As expected, USCL-P_{Cat}1 was found to populate a PPII helical structure even though it only has four proline residues. It was found to have a strong negative CD signal at 202 nm and positive CD signal at 225 nm which are characteristic features of a PPII secondary structure (Tiffany and Krimm 1968b; Ronish and Krimm 1974). The addition of an amino group in proline at the γ-carbon position and the acylation of the peptide N-terminus with palmitic acid do not seem to affect the conformation that USCL-P_{Cat}1 adopts in water at neutral pH as the CD spectrum, at 500 μM concentration, shows the expected PPII CD spectrum. On the other hand, its flexible counterpart, USCL-Dab1, was found to be in a disordered conformation, previously referred as a random coil, as we observed a negative CD bands at 197 nm. Interestingly, USCL-K1 is found to have significant PPII content as shown by its positive CD signal at 219 nm. It was first observed by Tiffany and Krimm (1968a) that long poly-L-lysine peptides in aqueous solution possess a left-handed helical structure. In addition, short tri-L-lysine peptides have been reported to form similar structure as their longer counterpart (Eker et al. 2004). Recently, it has been elucidated that poly-L-lysine forms a mixture of PPII and a novel left-handed 2.5_1-helical conformation, which is an extended β-strand-like conformation, in water using UV resonance Raman (UVR) spectroscopy (Mikhonin et al. 2005). Our data are in agreement with these observations and confirm that acylation of the N-terminus with palmitic acid does not affect the secondary structure of the USCLs. The representative USCLs were also ran at a lower concentration of 50 μM and found no difference in their CD profile (in comparison to 500 μM).

The stability of the USCL-P_{Cat}1 PPII structure was assessed over a range of pH's (Fig. 3) and temperatures (Fig. 4). We found that the structure, having only four P_{Cat} residues, is stable to wide pH and temperature changes. We observed a bathochromic (red) shift and a slight reduction of ellipticity at a basic pH of 11.3, in comparison to the acidic pH of 3.6 and neutral pH of 6.4. One helical turn in a PPII helix consists of three amino acid residues. Therefore, in the USCL-P_{Cat}1 structure, the first and the fourth P_{Cat} residues would be in-line with one another. The amino group at the γ-carbon would be protonated at acidic and neutral pHs. Hence, the USCL-P_{Cat}1 PPII helical structure would experience an electrostatic repulsion from the first and fourth residues, serving as an interlocking force, rendering the structure more rigid. As the pH moves to basic, the amino group would be deprotonated and would exist in its neutral form, effectively removing the electrostatic repulsion from the structure. Relieving the electrostatic

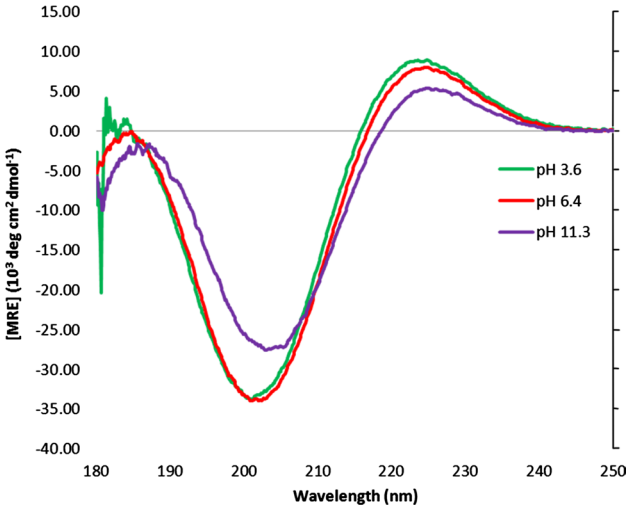

Fig. 3 Structural effects of pH on USCL-P_{Cat}1 in 10 mM phosphate buffer at 25 °C

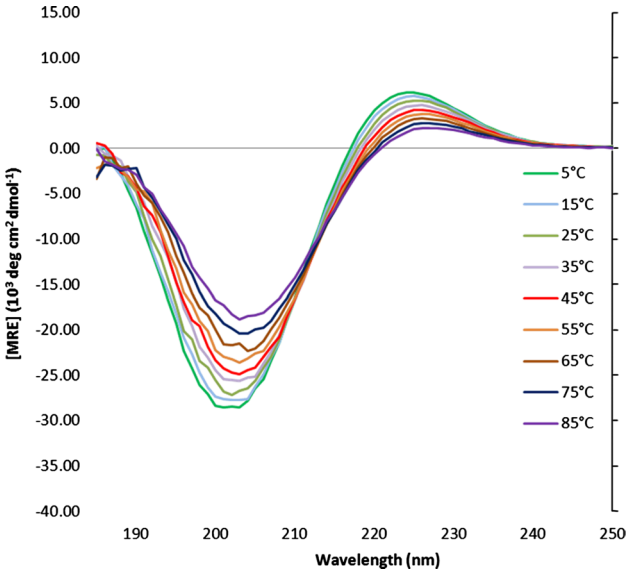

Fig. 4 CD spectrum for the thermal denaturation of USCL-P_{Cat}1 in 10 mM phosphate buffer at neutral pH from 5 to 85 °C

repulsion allows the peptide to sample more conformations in solution, resulting in the bathochromic shift and reduction of PPII CD signal at basic pH. The PPII helical structure is also stable over the temperature range of 5–85 °C with observed loss of molar ellipticity as temperature goes higher that is indicative of a reduction in PPII character.

Recently, Makovitzki et al. (2008) reported that some of their USCL adopt nanotubular structures while some forms micelles in aqueous solution. In contrast, the morphology of our synthesized USCLs (Fig. 5) was found to

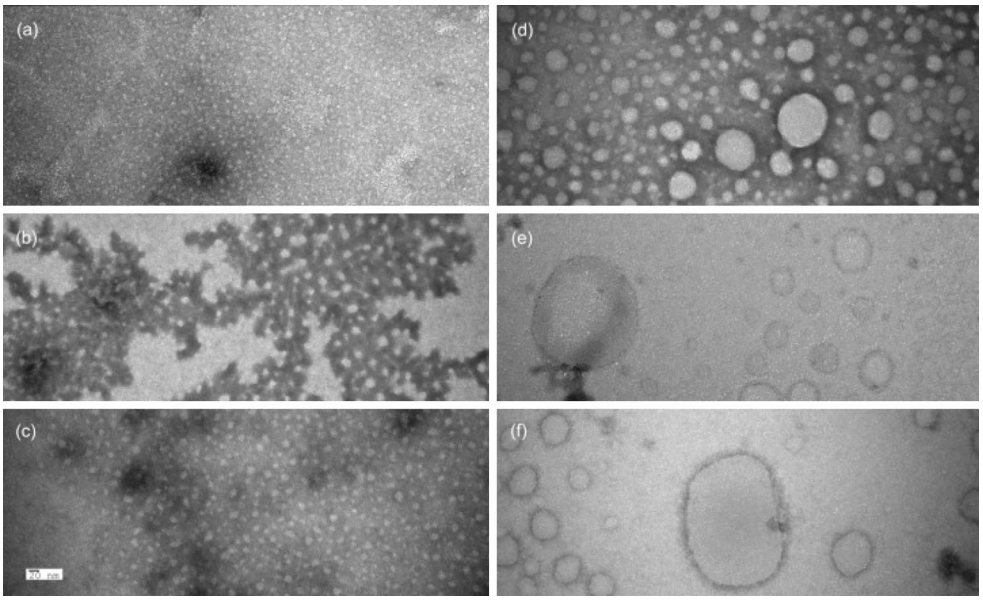

Fig. 5 Transmission electron microscopy images obtained for **a** USCL-K1, **b** USCL-Dab1, **c** USCL-P_{Cat}1, **d** USCL-K2, **e** USCL-Dab2 and **f** USCL-P_{Cat}2. Each of the USCLs at 200 μM concentration, immobilized on a carbon-coated copper grid, was stained using 1 % phosphotungstic acid to visualize their morphology at 60,000X magnification

be micellar in solution. Interestingly, there are only a few differences between our designs: the number of amino acids (we have a tetramer while they have a trimer) and the presence of a natural hydrophobic residue (they contain L-glycine and L-leucine) in the peptide sequence. In that context, we found no resolvable morphology for USCL-P_{Cat}4, containing the unnatural hydrophobic amino acid P_{Hex}, even at our highest resolution capacity (data not shown in the paper). We observed changes in the micellar diameter between USCLs containing C16 (Fig. 5a–c) and C16OH (Fig. 5d–f), the former having a uniform diameter of 5–15 nm while the latter having a non-uniform diameter: 5–15, 50–65 and 90–120 nm. We suspect that the presence of a hydroxyl group at the end of the 16-carbon aliphatic carboxylic acid affects the micellar packing in solution leading into two scenarios: (I) the USCL can fold itself in order for the hydroxyl group to interact with the polar peptide head group followed by micelle formation with other similarly folded molecules or (II) the USCL interacts with other molecules forming a pseudo lipid bilayer, having both polar ends interacting with the aqueous environment. It is most likely that both scenarios take place in the solution resulting in the smaller diameter micelles from scenario (I) while the larger diameter micelles result from scenario (II). Nonetheless, the amphipathicity of our synthesized USCLs renders them to adopt micellar structures in aqueous solutions. We observed no appreciable differences in the solution morphology between flexible (Fig. 5b, e) and ring-constrained (Fig. 5c, f) USCLs.

Antimicrobial activity

The susceptibility of standard laboratory reference and clinically isolated strains from CAN-ICU (Zhanel et al. 2008) and CANWARD studies (Zhanel et al. 2010, 2013) was tested in vitro against the synthesized USCLs to assess their minimum inhibitory concentration (MIC) values (Table 2). Direct comparison between the flexible USCL-Dab1 and its ring-constrained analog USCL-P_{Cat}1 demonstrated a fourfold greater MIC for the latter, suggesting that constraining the amino acid component is not beneficial for the USCL design. This observation was also observed for USCL-Dab3 against USCL P_{Cat}3, while no direct conclusion could be obtained from the comparison of USCL-Dab2 against USCL-P_{Cat}2 since both of these agents were not particularly active against tested strains. The addition of C16OH instead of C16, to impose disturbance within the USCL hydrophobic domain, was observed to decrease (if not abolish) the antibacterial activity of USCLs, as shown by the comparison of USCL-K1 against USCL-K2, USCL-Dab1 against USCL-Dab2 and USCL-P_{Cat}1 against USCL-P_{Cat}2. Interestingly, USCL-P_{Cat}4, where P_{Hex} was added to increase hydrophobicity in the peptide head portion of the design, demonstrated antimicrobial activity only against Gram-positive strains (*S. aureus* and MRSA). We suspect that the overall hydrophobicity of USCL-P_{Cat}4, coming from the C16 lipid tail and the hexyl side chain of P_{Hex}, is above the hydrophobic threshold needed for activity resulting in an impaired ability to penetrate or interact with the outer and/or cell membrane of Gram-negative bacteria.

Table 2 Antibacterial susceptibility of various microbes against synthesized USCL

Control organism	MIC [MIC with 4 % BSA] (μg/mL)								
	USCL-K1	USCL-Dab1	USCL-P_{Cat}1	USCL-K2	USCL-Dab2	USCL-P_{Cat}2	USCL-Dab3	USCL-P_{Cat}3	USCL-P_{Cat}4
S. aureus[a]	8 [512]	8 [256]	32 [>512]	128 [512]	64 [256]	256 [>512]	16 [> 128}	64 [> 512]	32 [512]
MRSA[b]	16 [512]	8 [512]	32 [>512]	128 [512]	64 [512]	256 [>512]	16 [> 128]	64 [> 512]	32 [512]
MSSE[c]	4 [256]	4 [128]	16 [512]	NT [NT]	NT [NT]	NT [NT]	8 [> 128]	32 [> 512]	NT [NT]
MRSE[d]	4 [256]	4 [128]	16 [512]	NT [NT]	NT [NT]	NT [NT]	8 [> 128]	32 [> 512]	NT [NT]
E. faecalis[e]	16 [512]	8 [512]	32 [512]	NT [NT]	NT [NT]	NT [NT]	16 [>128]	32 [>512]	NT [NT]
E. faecium[f]	8 [512]	8 [256]	16 [512]	NT [NT]	NT [NT]	NT [NT]	16 [NT]	32 [>512]	NT [NT]
S. pneumoniae[g]	64 [32]	32 [16]	64 [64]	NT [NT]	NT [NT]	NT [NT]	64 [256]	128 [64]	NT [NT]
E. coli[h]	8 [512]	8 [256]	32 [512]	256 [512]	128 [512]	512 [>512]	8 [>128]	32 [512]	512 [512]
E. coli[i]	8 [512]	16 [512]	32 [>512]	NT [NT]	NT [NT]	NT [NT]	16 [NT]	64 [>512]	NT [NT]
E. coli[j]	16 [512]	16 [512]	32 [>512]	NT [NT]	NT [NT]	NT [NT]	16 [NT]	32 [>512]	NT [NT]
E. coli[k]	8 [512]	16 [512]	32 [>512]	NT [NT]	NT [NT]	NT [NT]	8 [>128]	32 [>512]	NT [NT]
P. aeruginosa[l]	16 [>512]	8 [256]	256 [>512]	512 [>512]	256 [>512]	>512 [>512]	32 [>128]	128 [>512]	512 [512]
P. aeruginosa[m]	64 [512]	64 [256]	128 [512]	NT [NT]	NT [NT]	NT [NT]	64 [NT]	128 [>512]	NT [NT]
P. aeruginosa[n]	32 [>512]	16 [512]	256 [>512]	NT [NT]	NT [NT]	NT [NT]	32 [>128]	128 [>512]	NT [NT]
S. maltophilia[o]	256 [>512]	256 [>512]	256 [>512]	NT [NT]	NT [NT]	NT [NT]	128 [NT]	128 [>512]	NT [NT]
A. baumannii[p]	256 [>512]	256 [>512]	256 [>512]	NT [NT]	NT [NT]	NT [NT]	64 [NT]	128 [>512]	NT [NT]
K. pneumoniae[q]	32 [>512]	16 [512]	128 [>512]	NT [NT]	NT [NT]	NT [NT]	32 [NT]	128 [>512]	NT [NT]

MIC minimum inhibitory concentration, *BSA* bovine serum albumin, *MRSA* methicillin-resistant *S. aureus*, *MSSE* methicillin-susceptible *S. epidermidis*, *MRSE* methicillin-resistant *S. epidermidis*, *NT* not tested

[a] ATCC 29213

[b] ATCC 33592

[c] CANWARD-2008 81388

[d] CAN-ICU 61589—Ceftibuten resistant (MIC >32 μg/mL)

[e] ATCC 29212

[f] ATCC 27270

[g] ATCC 49619

[h] ATCC 25922

[i] CAN-ICU 61714—Gentamicin resistant

[j] CAN-ICU 63074—Amikacin resistant (MIC = 32 μg/mL)

[k] CANWARD-2011 97615—gentamicin resistant, tobramycin resistant, ciprofloxacin resistant, aminoglycoside modifying enzyme aac(3′)iia present

[l] ATCC27853

[m] CAN-ICU 62308—gentamicin resistant

[n] CANWARD-2011 96846—gentamicin resistant, tobramycin resistant

[o] CAN-ICU 62584

[p] CAN-ICU 63169

[q] ATCC 13883

The flexible USCL-Dab1 and USCL-Dab3, as well as the reference USCL-K1, demonstrated modest activity (MICs of 4–16 μg/mL) against both Gram-positive and Gram-negative strains, with the exception of the opportunistic pathogens *S. maltophilia* and *A. baumannii*. The three USCLs demonstrated promising antibacterial activity against a clinically isolated strain of multidrug resistant *E. coli*, resistant to gentamicin, tobramycin and ciprofloxacin. They were also active against *P. aeruginosa*, an opportunistic nosocomial Gram-negative pathogen characterized by intrinsic resistance to a wide-array of structurally different antibiotics via mechanisms including drug efflux pumps and a variety of chromosomally and plasmid-encoded resistance genes. We tested the three flexible USCLs against three different strains of *P. aeruginosa*, one laboratory reference strain and two clinical strains (one of which is resistant to both gentamicin and tobramycin), and found that their antimicrobial activity remains unchanged.

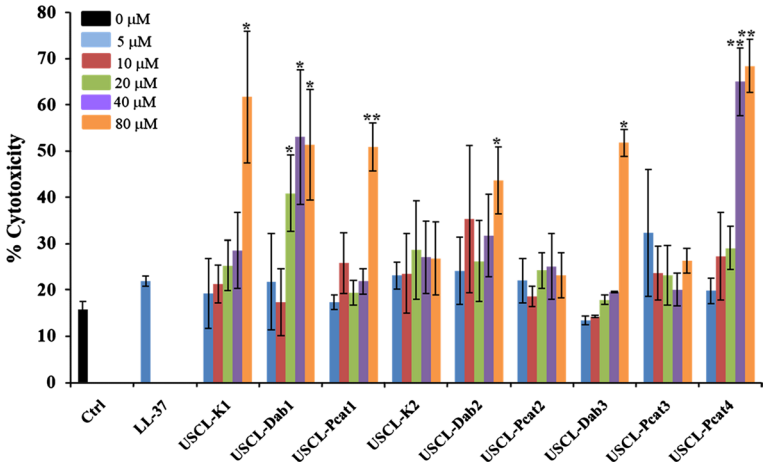

Fig. 6 Percent cytotoxicity of synthesized USCLs against human macrophage-like cells as measured by lactate dehydrogenase (LDH) release after 24 h incubation at 37 °C. Results are an average of three independent experiments ± standard error. Student's paired *t* test was used to evaluate significance compared to control unstimulated cells (*$p < 0.05$, **$p < 0.01$)

USCL-Dab1 and USCL-K1 showed good activity (MIC of 4 μg/mL) against methicillin-susceptible *S. epidermidis* (MSSE) and methicillin-resistant *S. epidermidis* (MRSE), both clinically isolated strains.

The antimicrobial testing was repeated with 4 % BSA to simulate protein binding in serum. As we previously reported with lipopeptides (Findlay et al. 2012a) and lipopeptoids (Findlay et al. 2012b), the presence of serum dramatically reduces the activity of USCL. This is attributed to the hydrophobic interactions of the protein with the hydrophobic domain of the lipopeptide, preventing the drugs from reaching their target (Svenson et al. 2007).

Cytotoxicity

To address the cytotoxicity of the synthesized compounds to mammalian immune cells, we stimulated macrophage-like differentiated monocytic THP-1 cells with the USCLs. Cytotoxicity was evaluated by monitoring lactate dehydrogenase release in tissue culture supernatants after 24 h stimulation (Fig. 6). We tested several USCL concentrations from 5 μM up to 80 μM and saw no appreciable cytotoxicity (less than 20 % cytotoxicity after the control is subtracted) until 20–40 μM range, concentrations that are typically used in preclinical murine models of infection (Scott et al. 2007). USCL-K2 and USCL-P_{Cat}2, both having a C16OH lipid tail, showed less than 20 % cytotoxicity even at a very high concentration of 80 μM. On the other end, USCL-P_{Cat}4 exhibited more than 50 % toxicity (after the control is subtracted) at 40–80 μM concentrations, possibly due to its overall hydrophobicity. Interestingly, USCL-P_{Cat}1 showed less toxicity in comparison to its flexible counterpart USCL-Dab1. This trend is also observed with USCL-P_{Cat}2 against USCL-Dab2. On the other hand, the comparison of USCL-Dab3 against USCL-P_{Cat}3 contradicted the trend where the flexible counterpart containing Dab and HSe was less toxic than the ring-constrained USCL. With these data presented, we have shown that the cytotoxicity of the USCLs is sequence-specific and ring constraint might not be the only factor to take into account in predicting its toxicity. It should be noted that 5 μM human cathelicidin LL-37 (also shown on Fig.6) was also tested for its cytotoxicity, and consequently for its cytokine and chemokine induction, as a comparison of our synthesized USCLs to a well-studied immunomodulatory host defence peptide.

Cytokine induction

The possibility of USCLs to induce beneficial immune responses, in particular chemokines that recruit leukocytes to the site of infections required for bacterial clearance was evaluated. Production of pro-inflammatory cytokines TNF-α and IL-1β, and chemokines IL-8 and Gro-α was monitored in tissue culture supernatants following stimulation of macrophage-like differentiated THP-1 cells with USCLs by ELISA. Our research group previously reported that some USCLs selectively induce the production of the chemokine IL-8 and Gro-α in significantly high amount (Findlay et al. 2013). Our newly synthesized USCLs did not induce the production of either pro-inflammatory cytokines TNF-α or IL-1β, or chemokines IL-8 or Gro-α (data not shown). On a positive note, our compounds did not induce the production of the two pro-inflammatory cytokines, which at a sustained elevated concentration could potentially escalate the inflammatory immune response during an infection, possibly resulting in septic shock. However, the compounds also did not induce significant production of chemokines IL-8 and Gro-α. Immunomodulatory antimicrobial (host defence) peptides such as the human cathelicidin LL-37 are known to induce both neutrophil and monocytic chemokine production, thus playing a critical role in leukocyte recruitment to the site of infection required for enhanced bacterial clearance (Mookherjee and Hancock 2007). Unfortunately,

our data show that our synthesized USCL may not be able to mediate immunomodulatory responses required for resolution of infections.

Conclusion

In summary, 9 USCLs were synthesized to directly compare the effects of having a flexible or a ring-constrained amino acid in the USCL design. The secondary structure of the representative USCLs in water and at 27 °C was elucidated using CD. USCL-P_{Cat}1, having only four L-4*R*-aminoproline residues, was found to populate a PPII helix while its flexible counterpart, USCL-Dab1, was found to be in a disordered conformation. Interestingly, USCL-K1, containing four L-lysine residues, showed a significant PPII helical content based on its CD spectra. The PPII structure of USCL-P_{Cat}1 was found to be stable from pH 3.6–11.3 and from 5 to 85 °C. The solution morphology of the USCLs was then observed using TEM. We found that our synthesized USCLs exhibit micellar structure and that a non-uniform micellar diameter was obtained by replacing the C16 lipid tail by C16OH.

The antimicrobial activities of our USCL's were tested against a panel of reference and clinically obtained bacterial strains, ranging from susceptible to multidrug-resistant organisms. As a direct comparison with the USCL's MIC, we observed that a flexible amino acid is beneficial to the activity of the USCL in comparison to a ring-constrained amino acid (as shown by the comparison of USCL-Dab1 against USCL-P_{Cat}1 and USCL-Dab3 against USCL-P_{Cat}3). Furthermore, our study showed that disturbing the hydrophobic domain by replacing C16 with C16OH decreases (if not abolishes) the antimicrobial activity of the USCL, regardless of its peptide sequence. The antibacterial activity of all USCLs was significantly reduced in the presence of 4 % BSA due to the non-specific hydrophobic interactions between the lipid tail of USCL and the protein.

Cytotoxicity against mammalian immune cells was addressed by measuring the LDH release from macrophages after stimulation with the synthesized USCLs for 24 h. We found no appreciable cytotoxicity up to concentrations of 20–40 μM. Our compounds did not induce the production of the pro-inflammatory cytokines TNF-α and IL-1β, thus indicating that these compounds will not mediate an inflammatory response in blood-derived mononuclear cells. However, the synthesized compounds also did not induce significant production of chemokines IL-8 and Gro-α.

Acknowledgments This work was supported by the Natural Sciences and Engineering Research Council of Canada (NSERC) and the Manitoba Health Research Council (MHRC).

Conflict of interest The authors declare that they have no conflict of interest.

References

Adzhubei AA, Sternberg MJ (1993) Left handed polyproline II helices commonly occur in globular proteins. J Mol Biol 229:472–493

Adzhubei AA, Stemberg MJE, Makarov AA (2013) Polyproline-II helix in proteins: structure and function. J Mol Biol 425:2100–2132

Ahn M, Murugan RN, Jacob B, Hyun J-K, Cheong C, Hwang E, Park H-N, Seo J-H, Srinivasrao G, Lee KS, Shin SY, Bang JK (2013) Discovery of novel histidine-derived lipo-amino acids: applied in the synthesis of ultra-short antimicrobial peptidomimetics having potent antimicrobial activity, salt resistance and protease stability. Eur J Med Chem 68:10–18

Chan WC, White PD (2000) Fmoc solid phase peptide synthesis: a practical approach, 1st edn. Oxford University Press Inc., New York

Choe J (2012) Fewer drugs, more superbugs: strategies to reverse the problem. APUA Clin Newsl 30:16–19

Choi K-Y, Chow LNY, Mookherjee N (2012) Cationic host defence peptides: multifaceted role in immune modulation and inflammation. J Innate Immun 4:361–370

Eisenstein B, Hermsen ED (2012) Resistant infections: a tragic irony in modern medicine. APUA Clin Newsl 30:11–12

Eker F, Griebenow K, Cao X, Nafie LA, Schweitzer-Stenner R (2004) Tripeptides with ionizable side chains adopt a perturbed polyproline II structure in water. Biochemistry 43:613–621

Findlay B, Zhanel GG, Schweizer F (2010) Cationic amphiphiles, a new generation of antimicrobials inspired by the natural antimicrobial peptide scaffold. Antimicrob Agents Chemother 54:4049–4058

Findlay B, Zhanel GG, Schweizer F (2012a) Investigating the antimicrobial peptide 'window of activity' using cationic lipopeptides with hydrocarbons and fluorinated tails. Int J Antimicrob Agents 40:36–42

Findlay B, Szelemej Zhanel GG, Schweizer F (2012b) Guanidylation and tail effects in cationic antimicrobial lipopeptoids. PLoS One 7:e41141

Findlay B, Mookherjee N, Schweizer F (2013) Ultrashort cationic lipopeptides and lipopeptoids selective induce cytokine production in macrophages. PLoS One 8:e54280

Hancock RE, Scott MG (2000) The role of antimicrobial peptides in animal defenses. PNAS 97:8856–8861

Haney EF, Hunter HN, Matsuzaki K, Vogel HJ (2009) Solution NMR studies of amphibian antimicrobial peptides: linking structure to function? Biochim Biophys Acta 1788:1639–1655

Jabes D (2011) The antibiotic R&D pipeline: an update. Curr Opin Microbiol 14:564–569

Kang S-J, Kim D-H, Mishig-Ochir T, Lee B-J (2012) Antimicrobial peptides: their physicochemical properties and therapeutic application. Arch Pharm Res 35:409–413

Laverty G, McLaughlin M, Shaw C, Gorman SP, Gilmore BF (2010) Antimicrobial activity of short, synthetic cationic lipopeptides. Chem Biol Drug Des 75:563–569

Makovitzki A, Avrahami D, Shai Y (2006) Ultrashort antibacterial and antifungal lipopeptides. Proc Natl Acad Sci USA 103:15997–16002

Makovitzki A, Baram J, Shai Y (2008) Antimicrobial lipopolypeptides composed of palmitoyl di- and tricationic peptides: in vitro and in vivo activities, self-assembly to nanostructures, and a plausible mode of action. Biochemistry 47:10630–10636

Mikhonin AV, Myshakina NS, Bykov SV, Asher SA (2005) UV resonance raman determination of polyproline II, extended 2.51-helix, and β-sheet Ψ angle energy landscape in poly-L-lysine and poly-L-glutamic acid. J Am Chem Soc 127:7712–7720

Mookherjee N, Hancock RE (2007) Cationic host defence peptides: innate immune regulatory peptides as a novel approach for treating infections. Cell Mol Life Sci 64:922–933

Mookherjee N, Brown KL, Bowdish DM, Doria S, Falsafi R, Hokamp K, Roche FM, Mu R, Doho GH, Pistolic J, Powers JP, Bryan J, Brinkman FS, Hancock RE (2006) Modulation of the TLR-mediated inflammatory response by the endogenous human host defense peptide LL-37. J Immunol 176:2455–2464

Mookherjee N, Rehaume LM, Hancock RE (2007) Cathelicidins and functional analogues as antisepsis molecules. Expert Opin Ther Targets 8:993–1004

Nguyen LT, Haney EF, Vogel HJ (2011) The expanding scope of antimicrobial peptide structures and their modes of action. Trends Biotechnol 29:464–472

Owens NW, Stetefeld J, Lattová E, Schweizer F (2010) Contiguous *O*-galactosylation of 4*R*-hydroxy-L-proline residues forms very stable polyproline II helices. J Am Chem Soc 132:5036–5042

Ronish EW, Krimm S (1974) The calculated circular dichroism of polyproline II in the polarizability approximation. Biopolymers 13:1563–1571

Schneider T, Muller A, Miess H, Gross H (2013) Cyclic lipopeptides as antibacterial agents—potent antibiotic activity mediated by intriguing mode of actions. Int J Med Microbiol 304:37–43

Scott MG, Dullaghan E, Mookherjee N, Glavas N, Waldbrook M, Thompson A, Wang A, Lee K, Doria S, Hamill P, Yu JJ, Li Y, Donini O, Guarna MM, Finlay BB, North JR, Hancock RE (2007) An anti-infective peptide that selectively modulates the innate immune response. Nat Biotechnol 25:465–472

Serrano GN, Zhanel GG, Schweizer F (2009) Antibacterial activity of ultrashort cationic lipo-β-peptides. Antimicrob Agents Chemother 53:2215–2217

Stanton TB (2013) A call for antibiotic alternatives research. Trends Microbiol 21:111–113

Steinstraesser L, Kraneburg U, Jacobsen F, Al-Benna S (2011) Host defense peptides and their antimicrobial-immunomodulatory duality. Immunobiology 216:322–333

Svenson J, Brandsdal BO, Stensen W, Svendsen JS (2007) Albumin binding of short cationic antimicrobial micropeptides and its influence on the in vitro bactericidal effect. J Med Chem 50:3334–3339

Thaker HD, Som A, Ayaz F, Lui D, Pan W, Scott RW, Anguita J, Tew GN (2012) Synthetic mimics of antimicrobial peptides with immunomodulatory responses. J Am Chem Soc 134:11088–11091

Tiffany ML, Krimm S (1968a) New chain conformations of poly(glutamic acid) and polylysine. Biopolymers 6:1379–1382

Tiffany ML, Krimm S (1968b) Circular dichroism of poly-L-proline in an unordered conformation. Biopolymers 6:1767–1770

Turner-Brannen E, Choi KY, Lippert DN, Cortens JP, Hancock RE, El-Gabalawy H, Mookherjee N (2011) Modulation of interleukin-1β-induced inflammatory responses by a synthetic cationic innate defence regulator peptide, IDR-1002, in synovial fibroblasts. Arthritis Res Ther 13:R129

Wayne PA, Clinical Laboratory Standards Institute (CLSI) (2006) Protocols for evaluating dehydrated Mueller–Hinton agar; approved standard. 2nd edn. Document M6-A2

Yeung ATY, Gellatly SL, Hancock RE (2011) Multifunctional cationic host defence peptides and their clinical applications. Cell Mol Life Sci 68:2161–2176

Yoneyama H, Katsumata R (2006) Antibiotic resistance in bacteria and its future for novel antibiotic development. Biosci Biotechnol Biochem 70:1060–1075

Zasloff M (1987) Magainins, a class of antimicrobial peptides from Xenopus skin—isolation, characterization of 2 active forms, and partial cDNA sequence of a precursor. Proc Natl Acad Sci USA 84:5449–5453

Zhanel GG, Adam HJ, Baxter MR, Fuller J, Nichol KA, Denisuik AJ, Lagace-Wiens PRS, Walkty A, Karlowsky JA, Schweizer F, Hoban DJ, on behalf of the Canadian Antimicrobial Resistance Alliance (CARA) (2013) Antimicrobial susceptibility of 22746 pathogens from Canadian hospitals: results of the CANWARD 2007–2011 study. J Antimicrob Chemother 68(Suppl 1):i7–i22

Zhanel GG, DeCorby M, Adam H, Mulvey MR, McCracken M, Lagace-Wiens P, Nichol KA, Wierzbowski A, Baudry PJ, Tailor F, Karlowsky JA, Walkty A, Schweizer F, Johnson J, The Canadian Antimicrobial Resistance Alliance (CARA), Hoban DJ (2010) Prevalence of antimicrobial resistant pathogens in Canadian hospitals: results of the Canadian ward surveillance study (CANWARD 2008). Antimicrob Agents Chemother 54:4684–4693

Zhanel GG, DeCorby M, Laing N, Weshnoweski B, Vashisht R, Tailor F, Nichol KA, Wierzbowski A, Baudry PJ, Karlowsky JA, Lagace-Wiens P, Walkty A, McCracken M, Mulvey MR, Johnson J, The Canadian Antimicrobial Resistance Alliance (CARA), Hoban DJ (2008) Antimicrobial resistant pathogens in intensive care units across Canada: results of the Canadian National Intensive Care Unit (CAN-ICU) Study, 2005/2006. Antimicrob Agents Chemother 52:1430–1437